The Astrophysical Journal Letters, 911:L14 (8pp), 2021 April 10 https://doi.org/10.3847/2041-8213/abee81

Accretion-modified Stars in Accretion Disks of Active Galactic Nuclei: Slowly Transient Appearance

Jian-Min Wang[1,2,3], Jun-Rong Liu[1,2], Luis C. Ho[4,5], and Pu Du[1]
[1] Key Laboratory for Particle Astrophysics, Institute of High Energy Physics, Chinese Academy of Sciences, 19B Yuquan Road, Beijing 100049, People's Republic of China
[2] School of Astronomy and Space Sciences, University of Chinese Academy of Sciences, 19A Yuquan road, Beijing 100049, People's Republic of China
[3] National Astronomical Observatory of China, 20A Datun Road, Beijing 100020, People's Republic of China
[4] Kavli Institute for Astronomy and Astrophysics, Peking University, Beijing 100871, People's Republic of China
[5] Department of Astronomy, School of Physics, Peking University, Beijing 100871, People's Republic of China
Received 2021 February 9; revised 2021 March 9; accepted 2021 March 12; published 2021 April 15

Abstract

Compact objects are expected to exist in the accretion disks of supermassive black holes (SMBHs) in active galactic nuclei (AGNs), and in the presence of such a dense environment ($\sim 10^{14}\,\mathrm{cm}^{-3}$), they will form a new kind of stellar population denoted as accretion-modified stars (AMSs). This hypothesis is supported by recent LIGO/Virgo detection of the mergers of very high-mass stellar binary black holes (BHs). We show that the AMSs will be trapped by the SMBH disk within a typical AGN lifetime. In the context of SMBH disks, the rates of Bondi accretion onto BHs are $\sim 10^{9} L_{\rm Edd}/c^{2}$, where $L_{\rm Edd}$ is the Eddington luminosity and c is the speed of light. Outflows developed from the hyper-Eddington accretion strongly impact the Bondi sphere and induce episodic accretion. We show that the hyper-Eddington accretion will be halted after an accretion interval of $t_{\rm a} \sim 10^{5} m_1\,\mathrm{s}$, where $m_1 = m_\bullet/10M_\odot$ is the BH mass. The kinetic energy of the outflows accumulated during $t_{\rm a}$ is equivalent to 10 supernovae driving an explosion of the Bondi sphere and developing blast waves. We demonstrate that a synchrotron flare from relativistic electrons accelerated by the blast waves peaks in the soft X-ray band ($\sim$0.1 keV), significantly contributing to the radio, optical, UV, and soft X-ray emission of typical radio-quiet quasars. External inverse Compton scattering of the electrons peaks around 40 GeV and is detectable through Fermi-LAT. The flare, decaying with $t^{-6/5}$ with a few months, will appear as a slowly varying transient. The flares, occurring at a rate of a few per year in radio-quiet quasars, provide a new mechanism for explaining AGN variability.

Unified Astronomy Thesaurus concepts: Active galactic nuclei (16)

1. Introduction

Compact objects (neutron stars and stellar black holes) may exist in accretion disks of active galactic nuclei (AGNs) and quasars. On the one hand, pioneering ideas of self-gravitating accretion disks in AGNs (Paczyński 1978; Kolykhalov & Sunyaev 1980; Shlosman & Begelman 1989) have received increasing attention (Collin & Zahn 1999, 2008; Goodman 2003; Goodman & Tan 2004; Wang et al. 2010, 2011, 2012), as they offer a possible explanation for the super-solar metallicities inferred in AGNs and quasars (Hamann & Ferland 1999; Warner et al. 2003; Nagao et al. 2006; Shin et al. 2013; Du & Wang 2014). The high metallicities can be naturally linked to star formation in self-gravitating disks, which inevitably produces compact objects from supernova explosions. On the other hand, the high metallicity of quasars can also be explained by stars from nuclear clusters captured by SMBH disks (Artymowicz et al. 1993), a process that will also introduce compact objects in the disks (Cheng & Wang 1999; Cantiello et al. 2021). Enveloped by the very dense gaseous medium of the accretion disk, compact objects inevitably will form a special kind of object, whose envelope is very massive, even more massive that the central compact object itself (see Section 2.2). We use the terminology of accretion-modified stars (AMSs) to denote them.[6] The fate of AMSs in such an environment, however, is unknown.

The recent detection of GW190521, consisting of $(85+66)M_\odot$ binary BHs, by the Advanced LIGO/Virgo consortium (Abbott et al. 2020) has received much attention because it is harbored by the quasar SDSS J1249+3449 monitored by the Zwicky Transient Facility (Graham et al. 2020). BH binaries with such high masses far exceeds the limit of pair instability of massive stars (e.g., Woosley 2017). As the BH masses of GW190521 are much higher than the upper limit of supernova explosions from an isolated star, this event has inspired the idea that mergers of compact objects can occur in AGN disks (Cheng & Wang 1999; Bartos et al. 2017; McKernan et al. 2019; Yang et al. 2019, 2020; Tanaga et al. 2020; Samsing et al. 2020). Such a scenario would involve AMSs in SMBH disks.

In this paper, we suggest that BHs are undergoing episodic accretion governed by powerful outflows developed from

[6] The classical Thorne–Żytkow objects (TZOs; Thorne & Żytkow 1975, 1977), which pertain to neutron stars enshrouded by envelopes, are in both hydrostatic and thermal equilibrium, with some accretion occurring just in the very inner region close to the neutron stars. They are expected to have specific surface abundances due to exotic nuclear burning processes happening deeper into the star and close to the compact object. The present AMSs are neither in hydrostatic nor thermal equilibrium. These compact objects are episodically accreting from the Bondi sphere.

hyper-Eddington accretion. The outflows drive a Bondi explosion and result in nonthermal flares from the blast waves that are predicted to appear as slowly varying transients in the radio, optical, UV, and soft X-ray bands. AMSs offer a new mechanism for explaining AGN variability but also for origins of massive stellar black holes.

2. A Simple Model

Stars, which originate either from capture from nuclear star clusters or direct formation from self-gravitating disks, accrete gas from SMBH disks to form more massive objects that evolve quickly into compact objects (Artymowicz et al. 1993; Cheng & Wang 1999; Cantiello et al. 2021). The massive envelope around a compact object forms an AMS through accretion of gas from the local SMBH disk. In this paper, we only focus on AMSs of black holes. Other more complicated options can arise.

The dimensionless accretion rate of the central SMBH is defined by $\dot{\mathscr{M}} = \dot{M}_\bullet/\dot{M}_{\rm Edd}$, where $\dot{M}_{\rm Edd} = L_{\rm Edd}c^{-2}$ is the Eddington limit rate, $\dot{M}_\bullet$ is the accretion rate of the SMBH, $L_{\rm Edd} = 4\pi GM_\bullet m_{\rm p}c/\sigma_{\rm T} = 1.3\times10^{46}M_8\ {\rm erg\ s^{-1}}$, G is the gravitational constant, $M_8 = M_\bullet/10^8M_\odot$ is the SMBH mass in units of $10^8M_\odot$, c is the speed of light, $m_{\rm p}$ is the proton mass, and $\sigma_{\rm T}$ is the Thomson cross section. The half-thickness, density, midplane temperature, and radial velocity of the SMBH disk are (e.g., Kato et al. 2008)

$$\begin{cases} H = 4.3\times10^{14}\,\alpha_{0.1}^{-1/10}M_8^{9/10}\dot{\mathscr{M}}^{3/20}r_4^{9/8}\ {\rm cm},\\ \rho_{\rm d} = 6.9\times10^{-11}\,(\alpha_{0.1}M_8)^{-7/10}\dot{\mathscr{M}}^{11/20}r_4^{-15/8}\ {\rm g\ cm^{-3}},\\ T_c = 4.6\times10^{3}\,(\alpha_{0.1}M_8)^{-1/5}\dot{\mathscr{M}}^{3/10}r_4^{-3/4}\ {\rm K},\\ v_r = 2.6\times10^{2}\,\alpha_{0.1}^{4/5}M_8^{-1/5}\dot{\mathscr{M}}^{3/10}r_4^{-1/4}\ {\rm cm\ s^{-1}}, \end{cases} \quad (1)$$

where $\alpha_{0.1} = \alpha/0.1$ is the viscosity parameter, $r_4 = R/10^4R_{\rm g}$ is the radius of the disk from the SMBH, and $R_{\rm g} = GM_\bullet/c^2$ is the gravitational radius. The self-gravity of the disk can be described by the Toomre parameter, defined as $Q = \Omega_{\rm K}c_s/\pi G\rho_{\rm d}H$, where $c_s \approx \sqrt{3kT_c/m_p} \approx 15.7\,T_4^{1/2}\ {\rm km\ s^{-1}}$ is the local sound speed of the SMBH disk and $\Omega_{\rm K} = \sqrt{GM_\bullet/R^3}$. The disk becomes self-gravitating (SG) beyond a critical radius, where $Q = 1$, which is given by

$$R_{\rm SG}/R_{\rm g} = 1.2\times10^3\,\alpha_{0.1}^{28/45}M_8^{-52/45}\dot{\mathscr{M}}^{-22/45}. \quad (2)$$

We consider the regions beyond $R_{\rm SG}$, where massive stars are formed either through capture by the SMBH disk or they are formed in situ, likely with a top-heavy initial mass function because of the high temperatures in the nuclear environment.

We would like to point out that the self-gravitating regions are undergoing more complicated physics beyond the solutions of Equation (1). For example, star formation is unavoidable (Collin & Zahn 1999, 2008; Sirko & Goodman 2003; Thompson et al. 2005), gravito turbulence dominates (Rafikov 2007, 2015), and the region has a clumpy distribution. The actual density and temperature could be different from that used here so that the fate of AMSs could be more complicated than currently assumed. The main characteristics of their evolution, however, can be predicted qualitatively. Future studies will be carried out about compact objects colliding with gaseous clumps in the self-gravitating regions.

2.1. AMSs

Considering that black holes formed from massive stars are kicked off with random velocities of $v_\bullet' \approx 10^2-10^3\ {\rm km\ s^{-1}}$ with respect to their remnant (the black holes are still tightly bound by the SMBHs), accretion onto the black holes in SMBH disks can be described by the Hoyle–Lyttleton–Bondi (HLB) formulation. Neglecting the weak dependence on adiabatic index and self-gravity of the accreted gas (Wandel 1984), we take the simplest form

$$\dot{M}_{\rm Bon} = \frac{4\pi G^2m_\bullet^2\rho_{\rm d}}{(c_s^2+v_\bullet^2)^{3/2}}, \quad (3)$$

where $m_\bullet$ is the black hole mass from supernova explosion and $v_\bullet$ is the kick-off velocity relative to the motion of the SMBH disk. The kick-off velocity of the black holes is uncertain, but it could be up to $v_\bullet' \sim 10^3\ {\rm km\ s^{-1}}$ if comparable with the case of neutron stars (e.g., Nakamura et al. 2019). We consider two extreme scenarios, in which the black hole is corotating and counterrotating with the SMBH disk. If $v_\bullet' \sim V_{\rm K} = 3000\,r_4^{-1/2}\ {\rm km\ s^{-1}}$, with $V_{\rm K}$ the Keplerian velocity, we expect two populations of accreting black holes in the disk: corotating black holes with $v_\bullet \approx |V_{\rm K} - v_\bullet'| \ll c_s$ and counterrotating ones with $v_\bullet \approx V_{\rm K} + v_\bullet' \approx 2V_{\rm K} \gg c_s$ (see Section 2.2). It should be stressed that the current choice of kick-off velocities are just for the two possible regimes, and is not necessarily representative of the bulk population. The corresponding accretion rates are

$$\dot{m}_{\rm Bon} = \frac{\dot{M}_{\rm Bon}}{\dot{M}_{\rm Edd}} \approx \begin{cases} 8.9\times10^8\,m_1(\alpha_{0.1}M_8)^{-2/5}\dot{\mathscr{M}}^{1/10}r_4^{-3/4} & \text{(for corotation)},\\ 5.1\,m_1(\alpha_{0.1}M_8)^{-7/10}\dot{\mathscr{M}}^{11/20}r_4^{-3/8} & \text{(for counter rotation)} \end{cases} \quad (4)$$

and the Bondi radius $R_{\rm Bon} = Gm_\bullet/(c_s^2+v_\bullet^2)$,

$$R_{\rm Bon} = \begin{cases} 1.2\times10^{15}\,m_1(\alpha_{0.1}M_8)^{1/5}\dot{\mathscr{M}}^{-3/10}r_4^{3/4}\ {\rm cm} & \text{(for corotation)},\\ 3.7\times10^9\,m_1r_4\ {\rm cm} & \text{(for counter rotation)}, \end{cases} \quad (5)$$

where $m_1 = m_\bullet/10M_\odot$ is the mass of the black hole inside the SMBH disk. The Hill radius is $R_{\rm Hill} = (M_{\rm Bon}/M_\bullet)^{1/3}R \approx 1.5\times10^{15}\,M_{\rm Bon,2}^{1/3}M_8^{2/3}r_4\ {\rm cm}$, which constrains the size of the AMS. Since $R_{\rm Bon} \approx R_{\rm Hill}$, tidal disruption of the AMS can be avoided. The validity of the HLB accretion is guaranteed by $R_{\rm Bon} \ll R_\rho$, where $R_\rho = |d\ln\rho_{\rm d}/dR|^{-1}$ is the density scale of the SMBH disk (i.e., the length that the density changes by an e-folding factor). A schematic illustrating an AMS embedded in an SMBH disk is shown in the left panel of Figure 1.

It should be noted that such a hyper-Eddington accretion is much higher than the case in the early universe, where seed black holes only attain a dimensionless accretion rate of $\dot{m}_\bullet \sim$ a few hundred (Volonteri & Rees 2005; Takeo et al. 2020; Toyouchi et al. 2021). Radiative feedback to the seed growth dominates in this case (Wang et al. 2006; Milosavljević et al. 2009a, 2009b; Regan et al. 2019). It depends on the Compton temperature, which in turn relies on the hard X-ray spectral slope. The slopes get steeper with increases of accretion rates

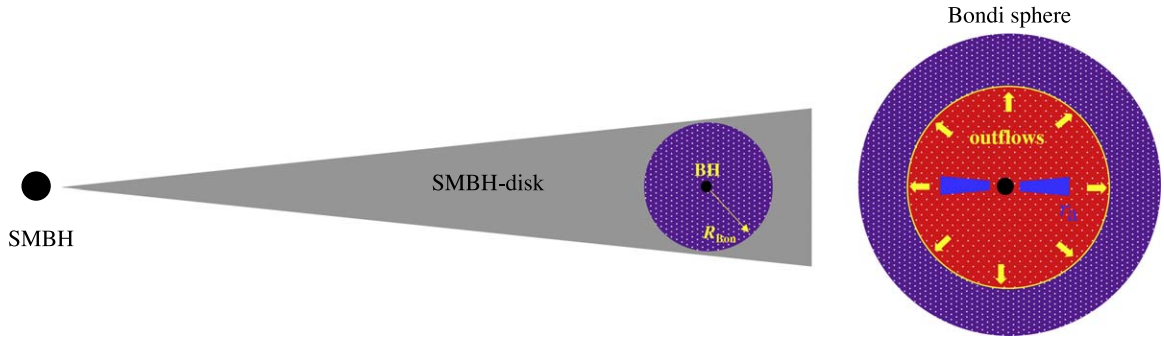

Figure 1. Left: stellar mass black holes ($1M_\odot$–$10^2M_\odot$) form accretion-modified stars (AMSs) to denote them in AGN accretion disks. Right: the Bondi sphere hosts a BH undergoing hyper-Eddington accretion. Powerful outflows developed from the slim disk of the BH produce strong feedback to the Bondi sphere. The hyperaccretion is halted by the mechanical feedback at the radius $r_a(\sim 10^4$ gravitational radii) within interval t_a, generating flares from radio to γ-rays (see the text for details). In this paper, we neglect the spins of the Bondi sphere (see a brief discussion in Section 2.2).

(Wang & Netzer 2003; Wang et al. 2004), lowering the Compton temperature. Moreover, luminosity saturation of the slim disk decreases the relative emission in hard X-rays (Abramowicz et al. 1988; Wang & Zhou 1999). Considering this fact, radiative feedback becomes weaker with increases of accretion rates. Radiative feedback could be still important for $\dot{m}_\bullet \sim 10^3$ from numerical simulations (Takeo et al. 2020), but mechanical feedback of outflows could dominate if $\dot{m}_\bullet \sim 10^9$ discussed in the current cases.

2.2. Friction on AMSs

The Bondi mass, which is defined as gas mass within the Bondi radius, can be approximated by $M_{\rm Bon} \approx 4\pi R_{\rm Bon}^3 \rho_{\rm d}/3$

$$M_{\rm Bon} = \begin{cases} 2.4 \times 10^2 M_\odot\, m_1^3 (\alpha_{0.1} M_8)^{-1/10} \dot{\mathscr{M}}^{-7/20} r_4^{3/8} & \text{(for corotation)}, \\ 7.3 \times 10^{-15} M_\odot\, m_1^3 (\alpha_{0.1} M_8)^{-7/10} \dot{\mathscr{M}}^{11/20} r_4^{9/8} & \text{(for counterrotation)}. \end{cases} \quad (6)$$

We note that the corotating AMSs are much more massive than those counterrotating. According to Equation (2) in Artymowicz et al. (1993), the drag force on an AMS parallel to its path is given by $F_{\rm d} = 4\pi G^2 M_{\rm AMS}^2 \rho_{\rm d} v_\bullet^{-2}$ for $v_\bullet < v_{\rm esc}$, where $v_{\rm esc} = \sqrt{2GM_{\rm AMS}/R_{\rm Bon}}$ is escaping velocity from the AMS surface, where $M_{\rm AMS} = M_{\rm Bon} + m_\bullet \approx (M_{\rm Bon}, m_\bullet)$ for corotating and counterrotating AMSs, respectively. Therefore, the slow-down timescale is given by $F_{\rm d} \times (v_\bullet t_{\rm slow}) = M_{\rm AMS} v_\bullet^2/2$, we have

$$t_{\rm slow} = \begin{cases} 14.2\, M_{\rm Bon,2}^{-1} \rho_{\bar{10}}^{-1} v_{100}^3 \ {\rm yr} & \text{(for corotation)}, \\ 3.8 \times 10^6\, m_1^{-1} \rho_{\bar{10}}^{-1} v_{3000}^3 \ {\rm yr} & \text{(for counterrotation)}, \end{cases} \quad (7)$$

where $v_{100,3000} = v_\bullet/(100, 3000)\,{\rm km\,s^{-1}}$, $\rho_{\bar{10}} = \rho_{\rm d}/10^{-10}\ {\rm g\ cm^{-3}}$. We find that the counterrotating AMSs need much longer times to slow-down than the corotating ones, and they have to spend a significant fraction of the typical AGN lifetime ($t_{\rm AGN} \sim R/v_r \sim 10^7\, r_4 v_2^{-1}$ yr, where $v_2 = v_r/10^2\,{\rm cm\,s^{-1}}$ from Equation 1). The randomly kicked BHs may leave the SMBH disk for some cases if $v_\bullet t_{\rm slow} \gtrsim H$, but they are still bound by the SMBH so that they are finally trapped by the disks. As fully random kick-off from supernova explosion, black holes, whose velocities perpendicular to the corotation direction will be dramatically damped according to Equation (7), and finally trapped by the SMBH disks.

Finally, we point out that the spin and angular momentum distribution of the AMSs are complicated issues. On the one hand, the accreted gas spins up the AMSs with an opposite direction to rotation of the SMBH disk since the AMS side near to the SMBH is rotating faster than its outside, namely AMS spins are from differential rotation of the disk. On the other hand, the tidal torque of the SMBH is still sufficiently strong to drive the AMS spin (at the characteristic radius $10^4 R_{\rm g}$), although the AMSs avoid the tidal disruption. The tidal torque drives the Bondi sphere to corotate with the disk when the Bondi sphere is large enough (like the case of the moon, whose spin follows its orbit around the Earth through the tidal torque of the Earth). Therefore, the outer part of the Bondi sphere generally has low spin because of the action of the negative tidal torque; however, the inner part may have some angular momentum where the torque is insufficiently strong. This could be the reason why there are slim accretion disks around the central black holes in the AMSs. This needs some detailed calculations for the AMSs as done for trapped stars in the SMBH disks by Jermyn et al. (2021), but it is beyond the scope of this paper.

2.3. Hyper-Eddington Accretion onto Black Holes

As shown by Equation (4), the black holes of AMSs have extremely high accretion rates ($\sim 10^9\, \dot{M}_{\rm Edd}$), which have never been discussed in the literature (except for accretion of neutrons onto black holes for γ-ray bursts). There are two schools of models of super-Eddington accretion onto black holes: (1) the classical model with so-called slim disks without outflows (Abramowicz et al. 1988; Wang & Zhou 1999) and (2) the model with accretion onto black holes with strong outflows (e.g., Ohsuga et al. 2005). Actual physics could fall between these two schools: photon trapping and outflows coexist (Kitaki et al. 2018). The first generally shows a cold disk with strong photon trapping. Simulations show that super-Eddington accretion produces powerful outflows strongly influencing its surroundings, but the midplane still continues accretion with rates from 300 to $10^3 L_{\rm Edd}/c^2$. The current accretion rates are higher than the cases discussed in Takeo et al. (2020) by five orders. We introduce two parameters in the BH accretion: (1) f_a as a fraction of the Bondi rates contributing to BH growth (Takeo et al. 2020) and (2) $f_{\rm out}(\sim 1)$ as a fraction of the Bondi rates to outflows. We have $\dot{m}_{\rm grow} = f_a \dot{m}_{\rm Bon}$.

The hyper-Eddington accreting black hole of the AMS has never been studied. In principle it should be a self-consistent system under the government of accretion and (radiative and

kinematic) feedback. When accretion rates are intermediately super-Eddington compared with the current context, such as $10^3 L_{\rm Edd}/c^2$, radiative feedback to its surroundings dominates and drives the accretion to be episodic (Wang et al. 2006; Milosavljević et al. 2009a, 2009b). If the hyper-Eddington accretion develops very powerful outflows with kinematic luminosity ($L_{\rm kin}$), for example, with a power of $\sim \dot{m} L_{\rm Edd}$, the kinematic momentum-driven feedback will dominate. The swept shell of the outflows follows (King 2003)

$$\frac{d}{dt}(M_r \dot{r}) = \frac{L_{\rm kin}}{v_{\rm out}}, \tag{8}$$

where M_r is the shell mass inside r and $v_{\rm out}$ is the velocity of the outflows. The kinematic luminosity during a single accretion episode is given by

$$L_{\rm kin} = \eta f_{\rm out} \dot{m}_{\rm Bon} L_{\rm Edd} = 1.3 \times 10^{47}\, \eta_{0.1} m_1 \dot{m}_9 \ {\rm erg\ s^{-1}}, \tag{9}$$

where $\dot{m}_9 = \dot{m}_{\rm Bon}/10^9$, η is the dissipating efficiency rather than the radiative efficiency and determined by the last stable orbit around black holes. Usually $\eta = 0.1$ is taken in the literature. The post-shock gas has a temperature $kT_{\rm sh} \approx 9 m_{\rm p} v_{\rm out}^2/16$, and accretion onto the BH is halted when $T_{\rm sh}$ is higher than the virial temperature $kT_{\rm vir} \approx m_{\rm p} c^2 (r/r_{\rm g})^{-1}$. We have the condition

$$v_{\rm out} = \frac{4}{3}\frac{c}{\sqrt{r_{\rm a}/r_{\rm g}}}, \tag{10}$$

to quench the accretion onto the black hole at a radius $r_{\rm a}$ of the slim disks. Integrating Equation (8), we have

$$M_r v_{\rm out} \approx \left(\frac{L_{\rm kin}}{v_{\rm out}}\right) t_{\rm a}, \tag{11}$$

where $t_{\rm a}$ is the accretion timescale. Here, we neglect the initial condition in the integration. Since the radial velocity of the hyper-Eddington accretion is $v_r = \alpha V_{\rm K}/\sqrt{5}$ (see Equation 11 in Wang & Zhou 1999), the accretion may be halted beyond $r_{\rm a}$ after

$$t_{\rm a} = \frac{r_{\rm a}}{v_r}. \tag{12}$$

Combining Equations (9)–(12), we have

$$\frac{r_{\rm a}}{r_{\rm g}} = \left(\frac{16\alpha}{9\sqrt{5}}\frac{M_{\rm Bon} c^3}{r_{\rm g} L_{\rm kin}}\right)^{2/5} = 1.3 \times 10^5\, \eta_{0.1}^{-2/5} \alpha_{0.1}^{13/25} M_8^{3/25} \dot{\mathscr{M}}^{-9/50} r_4^{9/20} \tag{13}$$

and

$$t_{\rm a} = \left(\frac{16\sqrt[3]{5}}{9}\frac{c^{4/3} r_{\rm g}^{2/3} M_{\rm Bon}}{\alpha^{2/3} L_{\rm kin}}\right)^{3/5} = 5.1 \times 10^4\, m_1 \eta_{0.1}^{-3/5} \alpha_{0.1}^{-11/50} M_8^{9/50} \dot{\mathscr{M}}^{-27/100} r_4^{27/40}\ {\rm s}, \tag{14}$$

where we take $M_r = M_{\rm Bon}$. The results show the necessary accretion timescale to quench the Bondi accretion through the outflows from slim accretion disks. $t_{\rm a}$ and $r_{\rm a}$ are not sensitive to the density distribution of the Bondi sphere. Figure 1 (right panel) shows a cartoon of the Bondi explosion driven by the powerful outflows from slim accretion disks with hyper-Eddington rates.

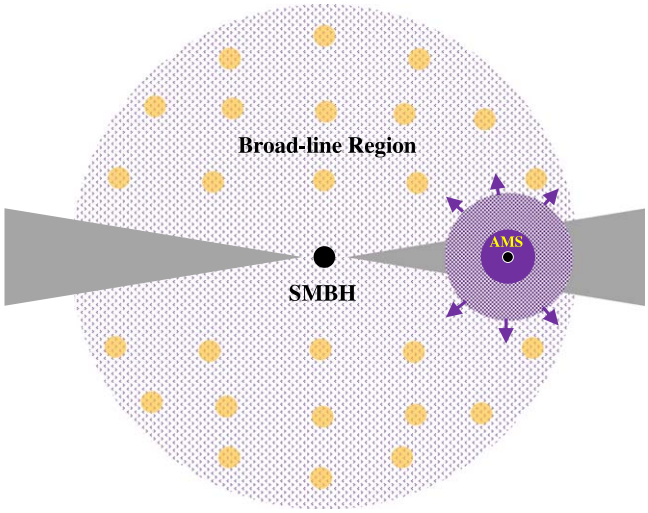

Figure 2. The Bondi explosion driven by the hyper-Eddington accretion onto the black hole of the (AMS). The plot is shown on a logarithmic scale. The explosion forms a cavity in the SMBH disk. The yellow balls are clouds in the broad-line region. The explosion propagates into the broad-line region with a density lower than that of the SMBH disk by a factor of 10^7, and thus it extends much beyond the disk. Such a violent explosion, equivalent to ∼10 supernovae, results in a slowly varying transient in many bands.

2.4. Bondi Explosion

The momentum-driven outflows are able to push the Bondi sphere within $t_{\rm a}$, but the cumulative kinematic energies during the period are much larger than the self-gravitational energy of the Bondi sphere so that it is undergoing explosion driven by cumulative energy of the outflows ($E_{\rm SG} \approx G M_{\rm AMS}^2/R_{\rm Bon} \approx 10^{48} M_{\rm AMS,2}^2 R_{\rm Bon,15}^{-1}$ erg $\ll E_{\rm kin}$). Figure 2 shows a cartoon of the Bondi explosion from an SMBH disk to the BLR. The cumulative kinematic energies within the sphere is

$$E_{\rm kin} = L_{\rm kin} t_{\rm a} = 1.3 \times 10^{52}\, \eta_{0.1} m_1 \dot{m}_9 t_{\rm a,5}\ {\rm erg}, \tag{15}$$

where $t_{\rm a,5} = t_{\rm a}/10^5$ s. We denote this as the Bondi explosion. Energies of one Bondi explosion are equivalent to that of about 10 supernovae. The explosion in the BLR (with medium density $\rho_{\rm BLR}$) as a quasi-sphere can be approximately described by the Sedov self-solution. However, the SMBH disk is not a sphere, so we use the adiabatic approximation for the expansion in the disk. Taking the SMBH disk as a slab, its opening solid angle to the Bondi sphere is about $\epsilon_{\rm d} \approx 0.5 (H/R_{\rm exp})^2$, where $R_{\rm exp}$ is the expanding radius of the Bondi explosion in the SMBH disk. Using the Sedov solution in BLR and the adiabatic approximation of $4\pi R_{\rm exp}^2 H n_{\rm d} k T_{\rm d} = \epsilon_{\rm d} E_{\rm kin}$ in the SMBH disk

$$R_{\rm exp} = \begin{cases} \left(\frac{E_{\rm kin}}{\rho_{\rm BLR}}\right)^{1/5} t^{2/5} = 55.1\, E_{52}^{1/5} n_{\rm BLR,7}^{-1/5} t_{10}^{2/5}\ {\rm ltd} & ({\rm for\ BLR\ medium}), \\ \left(\frac{H E_{\rm kin}}{8\pi n_{\rm d} k T_{\rm d}}\right)^{1/4} = 9.0 \times 10^{15}\, E_{52}^{1/4} \alpha_{0.1}^{1/5} M_8^{9/20} \dot{\mathscr{M}}^{-7/40} r_4^{15/16}\ {\rm cm} & ({\rm for\ SMBH-disk}), \end{cases} \tag{16}$$

the explosion velocity is

$$V_{\rm exp}=\begin{cases}\frac{2}{5}\left(\frac{E_{\rm kin}}{\rho_{\rm BLR}}\right)^{1/5}t^{-3/5}=1.8\times10^{3}\,E_{52}^{1/5}n_{\rm BLR,7}^{-1/5}t_{10}^{-3/5}\ {\rm km\ s^{-1}} & ({\rm for\ BLR\ medium}),\\ \left(\frac{2HL_{\rm kin}}{\pi n_{\rm d}kT_{\rm d}t_a^3}\right)^{1/4}=1.7\times10^{6}\,\alpha_{0.1}^{1/5}M_8^{9/20}\dot{\mathscr{M}}^{-7/40}r_4^{15/16}L_{47}^{1/4}t_{\rm a,5}^{-3/4}\ {\rm km\ s^{-1}} & ({\rm for\ SMBH-disk}),\end{cases}\tag{17}$$

from $4\pi R_{\rm exp}H(n_{\rm d}kT_{\rm d})V_{\rm exp}=\epsilon_{\rm d}L_{\rm kin}$ for SMBH disk, and the explosion timescale is

$$t_{\rm exp}=\begin{cases}\left(\frac{3}{4\pi}\right)^{5/6}\frac{M_{\rm Bon}^{5/6}}{\rho_{\rm BLR}^{1/3}E_{\rm kin}^{1/2}}=9.9\,M_{\rm Bon,2}^{5/6}n_{\rm BLR,7}^{-1/3}E_{52}^{-1/2}\ {\rm yr} & ({\rm for\ BLR\ medium}),\\ t_{\rm a}/2 & ({\rm for\ SMBH-disk}),\end{cases}\tag{18}$$

from the condition of $M_{\rm Bon}=4\pi R_{\rm exp}^2V_{\rm exp}\rho_{\rm BLR}t_{\rm exp}$, and $t_{\rm exp}=R_{\rm exp}/V_{\rm exp}$ for the SMBH disk, where $n_{\rm BLR,7}=n_{\rm BLR}/10^7\ {\rm cm^{-3}}$, $n_{\rm BLR}=\rho_{\rm BLR}/m_{\rm p}$, $E_{52}=E_{\rm kin}/10^{52}$ erg, $L_{47}=L_{\rm kin}/10^{47}\ {\rm erg\ s^{-1}}$, $t_{10}=t/10$ yr, $n_{14}=n_{\rm d}/10^{14}\ {\rm cm^{-3}}$, and $n_{\rm d}=\rho_{\rm d}/m_{\rm p}$ is the number density of the SMBH disk. The temperature of the shock-swept medium is

$$T\approx\frac{2(\Gamma_{\rm ad}-1)m_{\rm p}}{(1+\Gamma_{\rm ad})^2k}V_{\rm exp}^2=2.3\times10^{7}\,V_{\rm exp,3}^2\ {\rm K},\tag{19}$$

where $V_{\rm exp,3}=V_{\rm exp}/10^3\ {\rm km\ s^{-1}}$ and we take the adiabatic index $\Gamma_{\rm ad}=5/3$. It should be noted that the expansion velocity of the SMBH disk is relativistic and equivalent to a Lorentz factor $\Gamma_{\rm exp}\approx V_{\rm exp}/c\approx5$. A cavity with a radius $R_{\rm exp}$ is formed by the Bondi explosion in the SMBH disk. The small fraction $\epsilon_{\rm d}(\sim10\%)$ of $E_{\rm kin}$ could be thermalized in the SMBH disk, so we leave the relativistic blast waves as an open topic for the future. The Bondi explosion expands into the BLR medium.

Here we would like to stress that the above scenario of the Bondi explosion is the most conservative. The Bondi spheres are actually streaming toward the central black holes, leading to the possibility that the shocks can be enhanced through collision with the outflow. If we include radial self-gravity of the Bondi sphere (e.g., Wandel 1984), the shocks could be enhanced further. The streaming kinetic energy could be of the same order of magnitude as $E_{\rm SG}$; therefore, the characteristic features of the explosion remains. Additionally, it is interesting to compare the long γ-ray bursts (GRBs) and the Bondi explosion for the similarities and differences between them. Woosley (1993) pioneered an idea about the long GRBs. They originate from failed type Ib supernovae of massive stars; however, highly relativistic jets are developed from disk accretion of neutrons onto the central black holes with neutrino cooling. Their accretion rates, $\sim1\,M_\odot\ {\rm s^{-1}}\approx10^{15}\dot{M}_{\rm Edd}$, are much higher than the AMS cases. The similarity is that both kinds of explosions are driven by accretion onto black holes, but the differences rest on the fact that not only are cooling mechanisms distinguished but the GRBs are more violent in the extremely compact regions than the Bondi explosion. Unlike the GRBs dominated by relativistic jets, the Bondi explosions are driven by powerful outflows appearing as slow transients.

2.5. Rejuvenation of AMSs

The cavity formed by the Bondi explosion causes the BH to have very low accretion rates, and thus they are hardly detectable individually. However, the cold gas of the SMBH disk replenishes the cavity rejuvenating AMSs in a timescale of

$$t_{\rm rej}=\frac{R_{\rm exp}}{c_s}=268.9\,\alpha_{0.1}^{3/10}M_8^{11/20}\dot{\mathscr{M}}^{-13/40}r_4^{21/16}E_{52}^{1/4}\ {\rm yr}.\tag{20}$$

The duty cycle of the BH accretion is $\delta_\bullet=t_{\rm a}/(t_{\rm a}+t_{\rm rej})\approx6\times10^{-6}$. The episodic accretion efficiently constrains the BH growth. With the duty cycle, growth timescale is about $t_{\rm grow}=(\delta_\bullet\dot{m}f_{\rm a})^{-1}t_{\rm Salp}=10\,(\delta_{\bar5}\dot{m}_9f_{\rm a,\bar3})^{-1}\,t_{\rm Salp}$, where $t_{\rm Salp}=m_\bullet/\dot{M}_{\rm Edd}=0.45$ Gyr is the Salpeter time, $\delta_{\bar5}=\delta_\bullet/10^{-5}$, and $f_{\rm a,\bar3}=f_{\rm a}/10^{-3}$ is the fraction of the outflow to the accretion rates. The most uncertainty is in regards to $f_{\rm a}$, but it is easy for the BHs to grow up to $10^2M_\odot$ from $10M_\odot$. This requires numerical simulations of hyper-Eddington accretion at a small scale of $\lesssim10^3r_{\rm g}$.

It should be noted that most BHs are quiescent because of the extremely low duty cycles in SMBH disks. If they are in the sub-Eddington accretion status, they are radiating in X-ray bands like X-binaries. However, emissions from this kind of AMS (with a low accretion rate) depend on the details of its surroundings and its mass function. Total emissions of these accreting BHs may significantly contribute to the observations. This would be an interesting topic to explore in the future.

3. Observational Signatures of AMSs

3.1. Emissions from the Bondi Explosion

The Bondi explosion can be divided into two phases. First, internal shocks due to the collision between the outflows and the Bondi sphere. The dissipated energies could be of the orders of $E_{\rm SG}$ and channeled into thermal energy because of the very large optical depth $\tau_{\rm es}^0\approx\kappa_{\rm es}\rho_{\rm d}R\sim10^4$ for initial Bondi sphere with $R_{\rm Bon}\sim10^{15}$ cm and $\rho_{\rm d}\sim10^{-10}\ {\rm g\ cm^{-3}}$, where $\kappa_{\rm es}$ is electron scattering opacity. The optical depth of the expanding Bondi sphere is $\tau_{\rm es}\approx\kappa_{\rm es}(3M_{\rm Bon}/4\pi R^3)R\propto R^{-2}$, we find $\tau_{\rm es}=\tau_{\rm es}^0(R_{\rm Bon}/R)^2$. Since the Bondi explosion is mostly in the BLR medium, we neglect the part in the SMBH disk. When $R\sim10^2R_{\rm Bon}\sim10^{17}$ cm, this phase ends within an interval of $\delta t_{\tau_{\rm es}}\sim10^6$ s from Equation (16). We then have a variation of luminosity $\Delta L\sim E_{\rm SG}/\delta t_{\tau_{\rm es}}\approx10^{42}\ {\rm erg\ s^{-1}}$. This is too weak to observe for a quasar.

When $R=100R_{\rm Bon}$, the explosion begins to nonthermally radiate. For the simplest estimation, we assume that electrons

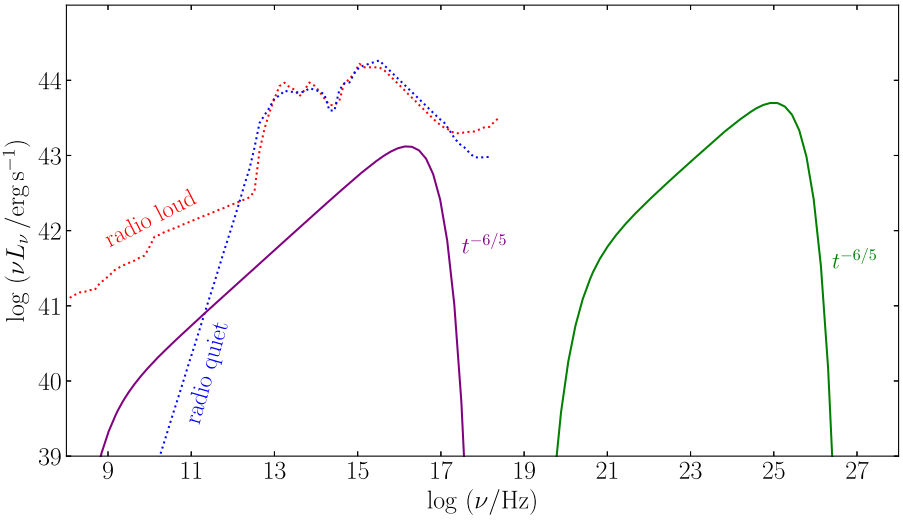

Figure 3. Spectral energy distributions (SEDs) of the Bondi explosion. Nonthermal emission from the explosion is characterized by SEDs peaking in the UV and TeV bands. Synchrotron emission is shown in purple, and external inverse Compton scattering is in green. The flare decays with time as $t^{-6/5}$, but the TeV photons are absorbed by pair production. We show the mean SEDs (Shang et al. 2011) of radio-quiet (dotted blue) and radio-loud (dotted red) quasars for $M_\bullet = 10^8 M_\odot$ and $\dot{\mathscr{M}} = 1$ (its bolometric luminosity of 10^{45} erg s^{-1}). We scale the mean quasar SED to match $L_{5100} \approx 0.1 L_{\rm bol}$. The luminosities at the synchrotron and inverse Compton peak frequency are $\sim 0.5(L_{\rm IC}, L_{\rm syn})$ for relativistic electrons with $n_e = 2$.

accelerated by shocks will generate nonthermal emissions with a fraction about ξ of $E_{\rm kin}$. For a giant flare of nonthermal emission with a luminosity of about $\Delta L \propto V_{\rm exp}^2$, we have

$$\Delta L_{\rm AGN} \approx L_0 \left(\frac{t}{t_{\rm es}}\right)^{-6/5} \ ({\rm for}\ t \geqslant t_{\rm es}), \tag{21}$$

from the self-similar expansion in the SMBH disk, where $L_0 = \xi E_{\rm kin}/5t_{\rm es} = 1.0 \times 10^{44}\, \xi_{0.05} E_{52} t_{\rm es,6}^{-1}$ erg s^{-1}, $\xi_{0.05} = \xi/0.05$ (e.g., Blandford & Eichler 1987), and $t_{\rm es,6} = t_{\rm es}/10^6$ s. L_0 is determined by the total energy of $\xi E_{\rm kin}$. Spectral energy distributions (SEDs) depend on relativistic electrons and surrounding photons (synchrotron radiation and inverse Compton scattering), but this is a significant contribution to the steady luminosity of quasars.

In order to show the characteristic of light curves, we assume that the shocks accelerate electrons to have a power law as $N_\gamma \propto \gamma^{-n_e}$ ($\gamma_{\rm min} \leqslant \gamma \leqslant \gamma_{\rm max}$) with an index n_e, where γ is the Lorentz factor of relativistic electrons. The maximum energy of an electron is determined by the balance between the acceleration and cooling. For the equipartition with the BLR hot phase, we have a magnetic field of $B \approx 0.6\, (n_7 T_7)^{1/2}$ G from $u_{\rm B} = n_{\rm BLR} k T_{\rm hot}$, where $u_{\rm B} = B^2/8\pi$ is energy density of the magnetic field and $T_{\rm hot} = 10^7 T_7$ is the temperature of the hot phase of the BLR. To illustrate the flare generated by the Bondi explosion, we consider a radio-quiet quasar with $M_\bullet = 10^8 M_\odot$ and $\dot{\mathscr{M}} = 1$. Its bolometric luminosity is $L_{\rm bol} = 1.3 \times 10^{45}\, \eta_{0.1} M_8 \dot{\mathscr{M}}$ erg s^{-1}. Photon energy density in the BLR is about $u_{\rm ph} = L_{\rm bol}/4\pi R^2 c \approx 0.16\, L_{45} R_{50}^{-2}$ erg cm^{-3} much higher than the magnetic fields, where $L_{45} = L_{\rm bol}/10^{45}$erg s^{-1}, $R_{50} = R/50$ ltd. This leads to external inverse Compton (IC) scattering as the dominant cooling of the relativistic electrons accelerated by shocks. Acceleration timescale is given by $t_{\rm acc} = R_{\rm L} c/V_{\rm exp}^2 \approx 5.8 \times 10^2\, \gamma_5 B_0^{-1} T_7^{-1}$ s (Blandford & Eichler 1987), while the inverse Compton cooling timescale is $t_{\rm IC} = 3 m_e c/4\sigma_{\rm T}\gamma u_{\rm ph} = 1.9 \times 10^3\, \gamma_5^{-1} u_{0.16}^{-1}$ s, where $R_{\rm L}$ is the Larmor's radius, $\gamma_5 = \gamma/10^5$, and $B_0 = B/1$ G. We have $\gamma_{\rm max} = 1.8 \times 10^5\, u_{0.16}^{-1/2} B_0^{1/2} T_7^{1/2}$ from $t_{\rm acc} = t_{\rm IC}$, and the maximum frequency of synchrotron and IC radiation are given by

$$\begin{aligned} \nu_{\rm syn}^{\rm max} &\approx 0.17\, B_0 \gamma_{\rm max,5}^2\ {\rm keV}, \\ \nu_{\rm IC}^{\rm max} &\approx \gamma_{\rm max}^2\, \nu_{\rm UV} \approx 41.7\, \gamma_{\rm max,5}^2 \nu_{15}^{\rm UV}\ {\rm GeV}, \end{aligned} \tag{22}$$

with the peak luminosities of

$$\begin{aligned} L_{\rm syn} &= 2.5 \times 10^{43} \left(\frac{u_{\rm B}/u_{\rm ph}}{0.25}\right) \left(\frac{L_{\rm IC}}{1 \times 10^{44}\ {\rm erg\ s^{-1}}}\right) {\rm erg\ s^{-1}}, \\ L_{\rm IC} &\approx 1 \times 10^{44}\, \xi_{0.05} E_{52} t_{\rm es,6}^{-1}\ {\rm erg\ s^{-1}}, \end{aligned} \tag{23}$$

for a spectral index of $L_\nu \propto \nu^{(1-n_e)/2}$, where $\nu_{15}^{\rm UV} = \nu_{\rm UV}/10^{15}$ Hz is the UV photon frequency from the SMBH disk. In Figure 3, we show the mean SED of a typical quasar in order to compare with multiwaveband light curves of the Bondi explosion.

From Figure 3, several remarkable features are found: (1) the synchrotron radiation peaks between soft X-rays (contributes to 1/3) and has significant contribution to optical and UV (about $\sim$0.1); (2) the Bondi explosion drives a radio-quiet quasar to become radio-intermediate in radio bands ($n_e = 2$); (3) the external inverse Compton peaks at $\sim$40 GeV, and with about 5×10^{43} erg s^{-1}, which can be detected in nonblazar AGNs by Fermi-LAT; (4) the transient appearance with a temporal profile as $t^{-6/5}$ and decaying a factor of 10 within about $6.8 t_{\rm es}$, namely, 3 months for $10^8 M_\odot$ quasars and the $10 M_\odot$ BH; (5) the intra-band emissions have no delays since they originate from the same regions. Moreover, for one BH with a few tens of solar mass, the above features will be more prominent. These characteristics are unique characteristics when identifying flares in AGNs.

Expansion of the Bondi explosion exhausts a small fraction of the total energy ($\sim$10%) in the SMBH disk, and most energy is released outside the disk as slow transients from radio to γ-rays. This is very different from that of the relativistic expansion driven by jets from neutron stars or black holes in SMBH disks discussed in Perna et al. (2021) and Zhu et al. (2021) (actually

for GRBs in the disks). Future detections of AGN light curves are useful to distinguish the nature of the AMSs in the SMBH disks.

3.2. Bondi Explosion Rates

According to the Kennicutt-Schmidt (KS) law of $\dot{\Sigma}_* = 2.5 \times 10^{-4}\Sigma_0^{1.4}\, M_\odot\ \mathrm{yr}^{-1}\,\mathrm{kpc}^{-2}$, star formation timescale is $t_* = \Sigma_0/\dot{\Sigma}_* = 4 \times 10^7\, \Sigma_5^{-0.4}$ yr, where $\Sigma_{0,5} = \Sigma_{\rm gas}/(10^0, 10^5)\, M_\odot\,\mathrm{pc}^{-2}$ is gas surface density of star formation regions. We note that t_* is comparable with $t_{\rm AGN}$. From Equation (1), we have surface density of SMBH disks of $\Sigma_{\rm disk} = 2.8 \times 10^8\, \alpha_{0.1}^{-4/5}\, M_8^{1/5}\, \dot{\mathscr{M}}^{7/10} r_4^{-3/4}\, M_\odot\mathrm{pc}^{-2}$, the KS law results in a rate of $\sim 2.5 M_\odot\ \mathrm{yr}^{-1}$ in the SMBH disk. This means that the KS star formation exhausts all disk gas in a timescale much shorter than $t_{\rm AGN}$ by a factor of 0.04. This is obviously inconsistent with observations of AGN lifetime. One way to overcome this inconsistency is to decrease the star formation efficiency or only a small fraction of SMBH disk mass converting into stars. Star formation in this region is poorly constrained by observations (e.g., Collin & Zahn 2008). For concreteness, we assume that the maximum star formation is that all SMBH disk gas is converted into stars with a rate of about $M_{\rm disk}/t_{\rm AGN}$, and black hole numbers are of $N_\bullet \sim M_{\rm disk}/\langle m_*\rangle$ over the AGN episode, where $M_{\rm disk} \approx 2\pi R^2 \Sigma_{\rm disk} = 4.4 \times 10^6\, \alpha_{0.1}^{-4/5} M_8^{11/5} \dot{\mathscr{M}}^{7/10} r_4^{5/4}\, M_\odot$. For a conserved consideration of star formation efficiency of $\zeta = 0.1$ in 10^8 yr (Kennicutt 1998), $\zeta M_{\rm disk}$ will be converted into stars $M_\star$, and a fraction of about $f_* = 10^{2(1-n_*)} \sim 0.1$ is massive stars for star formation with a top-heavy IMF (the maximum and minimum masses are (100, 1)$M_\odot$, $n_* = 0.5$ much more flattened than the Salpeter $n_* = 2.35$), where initial mass function $dN_* \propto m_*^{-n_*}$. According to stellar evolution theory (e.g., see Figure 16 in Woosley et al. 2002), about 10% stellar mass is converted into BHs (even high fraction to BHs) for $\langle m_*\rangle \sim 100 M_\odot$ stars (evolved within $t_{\rm AGN}$). The black hole numbers are about $N_\bullet \approx 4.4 \times 10^2\, \zeta_{0.1} f_{0.1} M_{\rm disk,6}/\langle m_*\rangle_2$, where $\langle m_*\rangle_2 = \langle m_*\rangle/10^2 M_\odot$, $\zeta_{0.1} = \zeta/0.1$ and $f_{0.1} = f_*/0.1$. Bondi explosion rates are about

$$\dot{\mathcal{R}}_{\rm Bondi} \approx \frac{N_\bullet}{t_{\rm rej}} \approx 1.6\, N_{\bullet,440} t_{\rm rej,270}^{-1}\ \mathrm{yr}^{-1}, \tag{24}$$

where $N_{\bullet,440} = N_\bullet/440$ and $t_{\rm rej,270} = t_{\rm rej}/270$ yr. The Bondi explosion drives one transient appearance per year. Considering the uncertainties of $N_\bullet$, such an event rate is also comparable to AGN giant flare rates. It would be very interesting to observationally test the real AGN flares. Additionally, AMSs with neutron stars or $\sim 1 M_\odot$ black holes have fainter flares than that of $10 M_\odot$ black holes; however, their numbers could be more and thus explosion rates could be higher than a few per year generating relatively stationary emissions. The correct answer to this problem depends on more sophisticated studies of the IMF and stellar evolution in the SMBH disks.

The Caltech-NRAO Stripe 82 Survey (CNSS), a dedicated radio transient survey (Mooley et al. 2016) to systematically explore the radio sky for slow transient phenomena on timescales between one day and several years, is very useful to detect the Bondi explosions suggested in this paper. The Very Large Array Sky Survey (VLASS) and Faint Images of the Radio Sky at Twenty (FIRST) cm survey, which have detected some variable objects (Nyland et al. 2020), are also very useful to test the present scenario. Moreover, the *Fermi*-LAT monitoring campaign of nonblazar AGNs also provides unique opportunities for testing the Bondi explosion mechanism proposed here. Indeed, several radio-quiet AGNs clearly show variability at >100 MeV (Sahakyan et al. 2018). Future joint radio and γ-ray observations of radio-quiet quasars have the potential to discover high-mass stellar black holes in SMBH disks.

3.3. Broad Emission Lines

Bondi explosions could not affect the broad-line region, which is composed of discrete clouds keeping a pressure balance with its surrounding medium. The shocked clouds will reach temperatures of up to $\sim 10^8$ K, but its free–free cooling timescale is about $t_{\rm ff}(\mathrm{BLR}) \approx 10^5\, T_8^{1/2} n_{10}^{-1}$ s, where $n_{10} = n_{\rm cloud}/10^{10}\,\mathrm{cm}^{-3}$ is the cloud density in the BLR. Since $t_{\rm ff}$(BLR) is much shorter than the timescale of the shock crossing the BLR ($t_{\rm BLR} = R_{\rm BLR}/V_{\rm exp} \sim 10^{8-9}$ s), the shocked clouds will recover rapidly. Thus, the BLR itself is not strongly affected by Bondi explosions.

4. Discussion and Conclusions

Compact objects evolved from massive stars remain inside the accretion disks of SMBHs in AGNs and quasars. They inevitably form AMSs in the extremely dense environment of SMBH disks. We suggest that the AMS black holes are episodically accreting with hyper-Eddington rates ($\sim 10^9 L_{\rm Edd}/c^2$) and duty cycles of $\sim 10^{-5}$. The active episodes are quenched by outflows from the hyper-Eddington accretion at a radius of $\sim 10^5$ gravitational radius of the AMS black holes. The episodic hyper-Eddington accretion allows stellar mass black holes to grow to exceed the well-known limit of the pair instability of massive stars. A powerful fireball produced by the outflows will drive an intense and fast expansion, which we call a Bondi explosion. Nonthermal flares from the Bondi explosion decay with a timescale of $t^{-6/5}$ for a few months, resulting in transient emission in the radio, optical, UV, soft X-ray, and GeV bands. With an occurrence rate of a few per year, Bondi explosions may contribute to the variable light curves of quasars.

Observational searches for AMSs should focus on slowly varying transients in radio-quiet AGNs as manifested in the radio, optical, UV, and γ-ray bands. Joint radio (e.g., CNSS and VLASS) and γ-ray (e.g., Fermi-LAT) observations would be promising. This Letter only outlines the fate of AMSs in SMBH disks, leaving much room for future investigations. Episodes of the BH accretion and the details of Bondi explosions should be more carefully studied through numerical simulations. The cavity in the SMBH disk formed by the Bondi explosion determines the rejuvenation of the AMS and the Bondi explosion rates. The nonthermal emission from the explosion should also be calculated more self-consistently.

The authors are grateful to an anonymous referee for a helpful report clarifying several points of the manuscript. J.M.W. especially thanks Bin Luo for useful information on CNSS results. Helpful discussions are acknowledged with Y.-R. Li and Y.-Y. Songsheng from IHEP AGN Group. J.M. W. thanks the support by National Key R&D Program of China through grant -2016YFA0400701 and -2020YFC2201400 by NSFC through grants NSFC-11991050, -11991054, -11833008, -11690024, and by grant No. QYZDJ-SSW-SLH007 and No. XDB23010400. L.C.H. is supported by the National Key R&D

Program of China through grant 2016YFA0400702 and the NSFC through grants 11721303 and 11991052. P.D. is supported by the NSFC through grants NSFC-12022301, -11991051, -11873048.

ORCID iDs

Jian-Min Wang https://orcid.org/0000-0001-9449-9268
Luis C. Ho https://orcid.org/0000-0001-6947-5846
Pu Du https://orcid.org/0000-0002-5830-3544

References

Abbott, R., Abbott, T. D., Abraham, S., et al. 2020, PhRvL, 125, 101102
Abramowicz, A., Czerny, B., Lasota, J.-P., et al. 1988, ApJ, 332, 646
Artymowicz, P., Lin, D., & Wampler, E. J. 1993, ApJ, 409, 592
Bartos, I., Kocsis, B., Haiman, Z., et al. 2017, ApJ, 835, 165
Blandford, R., & Eichler, D. 1987, PhR, 154, 1
Cantiello, M., Jermyn, A. S., & Lin, D. N. C. 2021, ApJ, 910, 94
Cheng, K. S., & Wang, J.-M. 1999, ApJ, 521, 502
Collin, S., & Zahn, J.-P. 1999, A&A, 344, 433
Collin, S., & Zahn, J.-P. 2008, A&A, 477, 419
Du, P., & Wang, J.-M. 2014, MNRAS, 438, 2828
Goodman, J. 2003, MNRAS, 339, 937
Goodman, J., & Tan, J. C. 2004, ApJ, 608, 108
Graham, M. J., Ford, K. E. S., McKernan, B., et al. 2020, PhRvL, 124, 251102
Hamann, F., & Ferland, G. 1999, ARA&A, 37, 487
Jermyn, A. S., Dittmann, A. J., Cantiello, M., & Perna, R. 2021, arXiv:2102.13114
Kato, S., Fukue, J., & Mineshige, S. 2008, Black Hole Accretion Disks (Kyoto: Kyoto Univ. Press)
Kennicutt, R. C., Jr. 1998, ARA&A, 36, 189
King, A. 2003, ApJL, 596, 27
Kitaki, T., Mineshige, S., Ohsuga, K., & Kawashima, T. 2018, PASJ, 70, 108
Kolykhalov, P. I., & Sunyaev, R. A. 1980, SvAL, 6, 357
McKernan, B., Ford, K. E. S., Bartos, I., et al. 2019, ApJL, 884, L50
Milosavljević, M., Bromm, V., Couch, S. M., et al. 2009b, ApJ, 698, 766
Milosavljević, M., Couch, S. M., & Bromm, V. 2009a, ApJL, 696, 146
Mooley, K. P., Hallinan, G., Bourke, S., et al. 2016, ApJ, 818, 105
Nagao, T., Maiolino, R., & Marconi, A. 2006, A&A, 447, 863
Nakamura, K., Takiwaki, T., & Kotake, K. 2019, PASJ, 71, 98
Nyland, K., Dong, D. Z., Patil, P., et al. 2020, ApJ, 905, 74
Ohsuga, K., Mori, M., Nakamoto, T., & Mineshige, S. 2005, ApJ, 628, 368
Paczyński, B. 1978, AcA, 28, 91
Perna, R., Lazzati, D., & Cantiello, M. 2021, ApJL, 906, L7
Rafikov, R. R. 2007, ApJ, 662, 642
Rafikov, R. R. 2015, ApJ, 804, 62
Regan, J. A., Downes, T. P., Volonteri, M., et al. 2019, MNRAS, 486, 3892
Sahakyan, N., Baghmanyan, V., & Zargaryan, D. 2018, A&A, 614, A6
Samsing, J., Bartos, I., D'Orazio, D. J., et al. 2020, arXiv:2010.09765
Shang, Z., Brotherton, M. S., Wills, B. J., et al. 2011, ApJS, 196, 2
Shin, J., Woo, J.-H., Nagao, T., et al. 2013, ApJ, 763, 58
Shlosman, I., & Begelman, M. C. 1989, ApJ, 341, 685
Sirko, E., & Goodman, J. 2003, MNRAS, 341, 501
Takeo, E., Inayoshi, K., & Mineshige, S. 2020, MNRAS, 497, 302
Tanaga, H., Haiman, Z., & Kocsis, B. 2020, ApJ, 898, 25
Thompson, T. A., Quataert, E., & Murray, N. 2005, ApJ, 630, 167
Thorne, K. S., & Żytkow, A. N. 1975, ApJL, 199, L19
Thorne, K. S., & Żytkow, A. N. 1977, ApJ, 212, 832
Toyouchi, D., Inayoshi, K., Hosokawa, T., & Kuiper, R. 2021, ApJ, 907, 74
Volonteri, M., & Rees, M. J. 2005, ApJ, 633, 624
Wandel, A. 1984, MNRAS, 207, 861
Wang, J.-M., Chen, Y.-M., & Hu, C. 2006, ApJL, 637, L85
Wang, J.-M., Du, P., Baldwin, J. A., et al. 2012, ApJ, 746, 137
Wang, J.-M., Ge, J.-Q., Hu, C., et al. 2011, ApJ, 739, 3
Wang, J.-M., & Netzer, H. 2003, A&A, 398, 927
Wang, J.-M., Watarai, K.-Y., & Mineshige, S. 2004, ApJL, 607, 107
Wang, J.-M., Yan, C.-S., Gao, H.-Q., et al. 2010, ApJL, 719, L148
Wang, J.-M., & Zhou, Y.-Y. 1999, ApJ, 516, 420
Warner, C., Hamann, F., & Dietrich, M. 2003, ApJ, 596, 72
Woosley, S. E. 1993, ApJ, 405, 273
Woosley, S. E. 2017, ApJ, 836, 244
Woosley, S. E., Heger, A., & Weaver, T. A. 2002, RvMP, 74, 1015
Yang, Y., Bartos, I., Gayathri, V., et al. 2019, PhRvL, 123, 181101
Yang, Y., Gayathri, V., Bartos, I., et al. 2020, ApJL, 901, L34
Zhu, J.-P., Zhang, B., Yu, Y.-W., et al. 2021, ApJL, 906, L11